

## Dynamic Toughness Fracture of some Metallic Materials (Probabilistic Aspects)

**REFERENCE** Tolba, B. and Pluinage, G., **Dynamic toughness fracture of some metallic materials (probabilistic aspects)**, *Defect Assessment in Components – Fundamentals and Applications*, ESIS/EGF9 (Edited by J. G. Blauel and K.-H. Schwalbe) 1991, Mechanical Engineering Publications, London, pp. 539–547.

**ABSTRACT** The increase of scatter in fracture tests performed at high loading rate suggests the need to analyse results in terms of statistical approach. Static and dynamic tests are presented with the well-known Weibull approach. The influence of the loading rate on the characteristic parameters of the probability of fracture toughness distribution is discussed.

### Notation

$C_w$	Constant
$K_{Ic}$	Fracture toughness
$KIc$	Average fracture toughness
$\dot{K}_I$	Stress intensity factor rate
$K_o$	Normalisation factor
$K_{min}$	Threshold value
$L$	Class width
$m$	Weibull shape parameter
$t_c$	Time to fracture
$V_a$	Variance
$\Gamma$	Gamma function

### Introduction

The increase of the loading rate leads to a modification of the fracture resistance. Two major facts appear:

- (i) the fracture toughness is generally reduced;
- (ii) scatter in tests is increased.

The decrease of fracture toughness can be satisfactorily explained by using a local fracture criterion and a model describing the change in the constitutive equation with temperature and loading rate. For steels, this has been done (1) using the Ritchie, Knott, and Rice (RKR) local fracture criterion and a model of thermally activated plasticity. For polymers, use of the generalised theory of

\* Université de Metz, Laboratoire de Fiabilité Mécanique, Ile du Saulay, 57045 Metz Cédex 01, France.

Table 1(a) Chemical composition of cast iron

Elements	C	Si	Mn	P	Mg	S
Weight (%)	3.47	1.96	0.07	0.045	0.030	0.006

Table 1(b) Mechanical properties of cast iron

Ultimate tensile strength (UTS) (MPa)	$K_{Ic}$ (MPa $\sqrt{m}$ )	Charpy 'V' impact value (CVN) (J)	A (%)	$\sigma_y$ (MPa)	Hardness (Brinell)
400-420	20-60	14	18-20	260-280	200

fracture combined with a model of time-temperature equivalence (2) has opened a promising way to solve this problem.

The second aspect of the influence of loading rate on fracture is an increase of the scatter of results. This leads to the conclusion that this phenomenon is a consequence of a change in the fracture process.

Table 2(a) Chemical composition of A 508 Cl 3

Elements	C	Mn	Ni	Mo	Si	Cr	Cu	Co	P	V	S
Weight (%)	0.16	1.3	0.7	0.51	0.25	0.2	0.08	0.02	0.01	0.01	0.004

Table 2(b) Mechanical properties of A 508 Cl 3 steel

Yield stress $\sigma_y$ (MPa)	Fracture stress $\sigma_{ul}$ (MPa)	Cleavage stress $\sigma_c$ (MPa)	Ultimate strain A (%)	Transition temperature $T_A$ (°C)
468-490	607-620	1585	20	-20

Table 3(a) Chemical composition of magnesium alloy GA 3Z1

Elements	A	Zn	Mn (min)	Si (max)	Cu (max)	Fe (max)	Ni (max)
Weight (%)	2.5-3.5	0.5-1.5	$\geq 0.2$	0.1	0.05	0.005	0.005

Table 3(b) Mechanical properties of magnesium alloy GA3Z1

Fracture stress $\sigma_f$ (MPa)	Ultimate stress $\sigma_{ul}$ (MPa)	Yield stress $\sigma_y$ (MPa)	Ultimate strain (%)
240-290	340-360	180-230	10-16

By measuring the fracture surface roughness, it can be noticed that this parameter decreases when increasing the loading rate. It has been shown, by using surface analysis on ceramics (3) that this phenomena is the consequence of a multi-defects activation fracture process; at low strain rate only the critical defect is activated.

In this paper, this problem is examined on three metallic materials broken at two loading rates, statically ( $\dot{K}_I = 1 \text{ MPa}\sqrt{m/s}$ ) and dynamically ( $\dot{K}_I = 10^6 \text{ MPa}\sqrt{m/s}$ ) using wedge loading CT (WLCT) samples ( $20 \times 20 \times 20 \text{ mm}$ ) and a Split Hopkinson Pressure Bar. The experimental device and sample's geometry are described in references (3) and (4). These three materials are a A 508 CL3 steel, a cast iron with spheroidized graphite and a magnesium alloy GA3Z1. The chemical composition and mechanical properties of these materials are presented in Tables 1-3. The method for dynamic fracture toughness determination was described previously (4).

## Experimental results

### Fracture toughness $K_{Ic}$ under static loading

It is necessary to define the average stress intensity factor rate  $K$  according to the following formula

$$\dot{K}_I = K_{Ic}/t_c \quad (1)$$

where  $t_c$  is the time to fracture for static tests performed according to the standard. The loading rate, the number of tests, and the test temperatures for the three materials are listed in Table 4.

For A 508 Cl 3 steel, an average value of  $56.51 \text{ MPa}\sqrt{m}$  has been obtained which is higher than the values found in the literature: (2) ( $47 \text{ MPa}\sqrt{m}$ ), (5) ( $37.5 \text{ MPa}\sqrt{m}$ ), (6) ( $40 \text{ MPa}\sqrt{m}$ ). Differences can be explained by different chemical composition and rolling conditions. For cast iron, the average value

Table 4 Static tests ( $\dot{K}_I$ , number of tests and temperature)

Materials	A 508 Cl 3	Cast iron	GA 3Z1
$\dot{K}_I$ (MPa $\sqrt{m/s}$ )	$\approx 1$	5.25	1.30
Number of tests (N)	14	36	45
Temperature (°C)	-196	20	20
Average Fracture Toughness $K_{Ic}$ (MPa $\sqrt{m}$ )	56.51	35.9	20.12
$K_o$ (MPa $\sqrt{m}$ )	59.04	36.8	20.80
m	11.60	21.48	16.03

is 35.9 MPa $\sqrt{m}$ . Our results can only be compared with results published on vermicular graphite cast iron. They are similar to those obtained on this material by Wilshaw *et al.* (7) (36 MPa $\sqrt{m}$ ), Spink *et al.* (8) (37 MPa $\sqrt{m}$ ). For the magnesium alloy GA 3Z1, the average value of 20.12 MPa $\sqrt{m}$  cannot be compared, since results on this material are relatively rare.

#### Fracture toughness $K_{Ic}$ under dynamic loading

For A 508 Cl 3 steel, the average dynamic fracture toughness is 76.43 MPa $\sqrt{m}$  at room temperature which is 10 percent higher than that obtained on the same material with the same equipment by Garnier (4). This difference may be attributed by some ambiguities with detection of crack initiation on dynamic tests. Comparison for dynamic tests is not possible for cast iron and magnesium alloy; no results at so high loading rate are available in literature. We can only mention that cast iron fracture toughness decreases of 6 percent when the loading rate increases from 5.25 MPa $\sqrt{m/s}$  to 10<sup>6</sup> MPa $\sqrt{m/s}$ . For magnesium alloy, the decrease is 15 percent for increasing loading rates from 1.3 MPa $\sqrt{m/s}$  to 2.10<sup>5</sup> MPa $\sqrt{m/s}$ . The particular case of steel has been seen previously (4) and increasing of fracture toughness at high loading rate attributed to some instability which appears on the stress-strain curve.

#### Comparison between static and dynamic loading

A decrease of fracture toughness for increasing loading rate has been observed by several authors, e.g., (4)(9)(10). In the case of steels, it is necessary to take into account the change of the transition temperature with loading rate.

For this reason only the brittle plateau has been compared at two different temperatures (20°C in the dynamic case, -196°C in the static one). Unfortunately, in the dynamic case we are not on the brittle plateau as we have expected but at the beginning of the transition foot. For this reason fracture toughness is greater in the dynamic case. For cast iron both values agree within the scatter, 32.8 MPa $\sqrt{m}$  and 36 MPa $\sqrt{m}$ . Only for GA 3Z1 is the dynamic toughness smaller than the static one (17.1 MPa $\sqrt{m}$  and 20.12 MPa $\sqrt{m}$ ).

#### Statistical treatment of experimental results

As mentioned previously, another aspect of the influence of the loading rate is the change in scatter. This particular aspect has been studied using the two parameters of Weibull's statistical approach.

The general (three parameters) Weibull type probability distribution function of  $K_{Ic}$  is given by

$$P(K_{Ic}) = 1 - \exp \left[ - \left\{ \frac{K_{Ic} - K_{min}}{K_0 - K_{min}} \right\}^m \right] \quad (2)$$

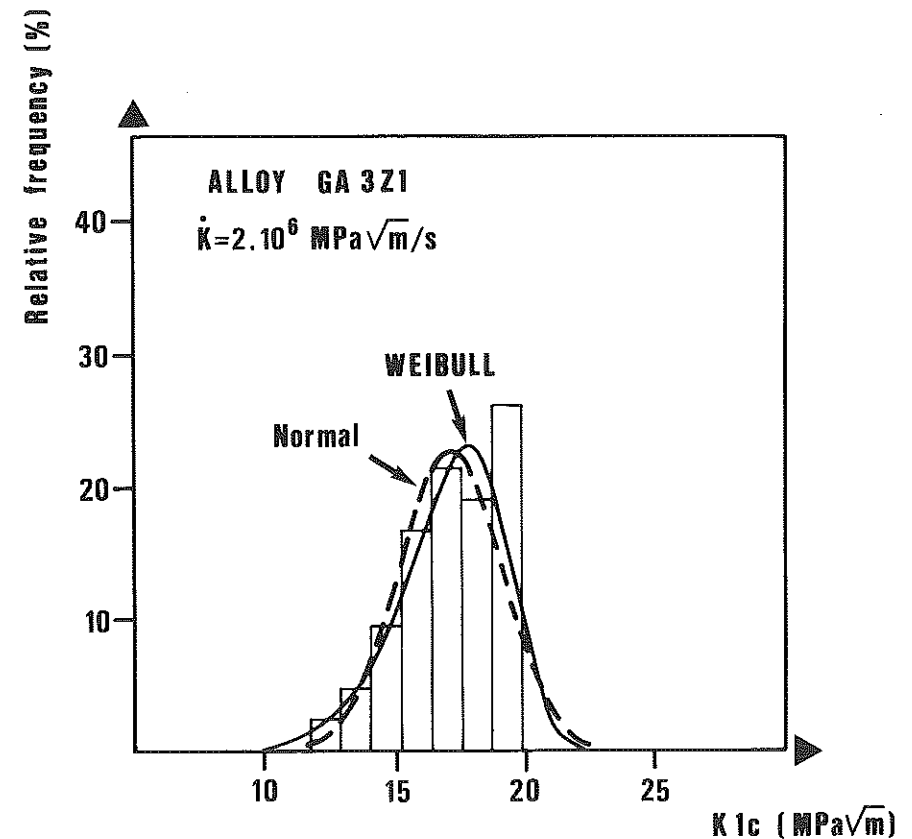


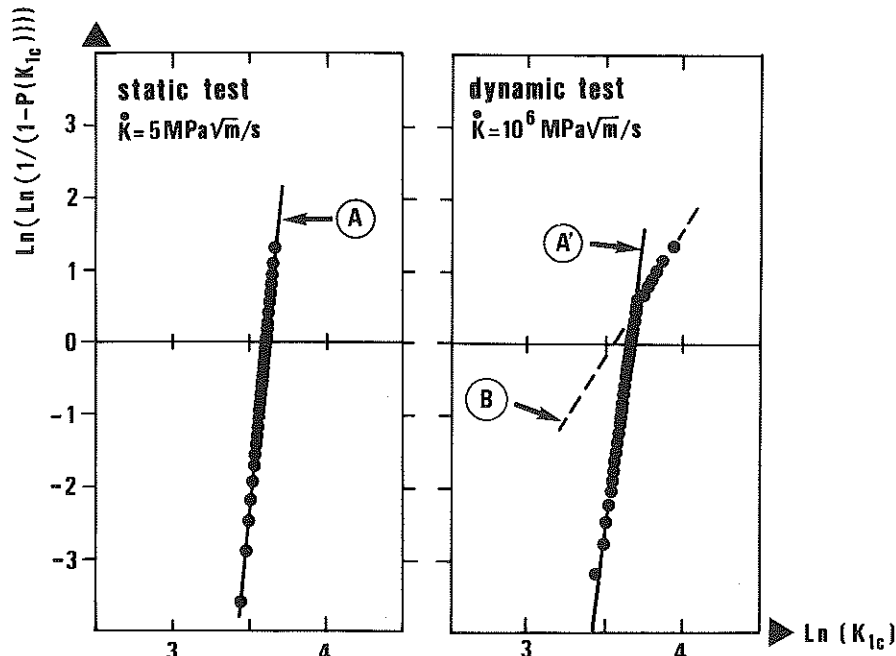
Fig 1 Relative frequency of  $K_{Ic}$  as compared with normal and Weibull probability density functions

$K_0$  is a normalisation factor and  $m$  the inhomogeneity factor or Weibull's modulus.

The fracture toughness threshold  $K_{min}$ , which is the value below which the probability of failure is equal to zero, is assumed to be zero ( $K_{min} = 0$ ) for

Table 5 Dynamic tests ( $\dot{K}_I$ , temperature and average fracture toughness)

Materials	A 508 Cl 3	Cast iron	GA3Z1
$\dot{K}_I$ (MPa $\sqrt{m/s}$ )	13.10 <sup>5</sup>	$\approx 10.10^5$	2.10 <sup>5</sup>
Temperature (°C)	20	20	20
Number of tests (N)	14	47	42
$K_{Ic}$ (MPa $\sqrt{m}$ )	76.43	38.16	17.10
$K_0$ (MPa $\sqrt{m}$ )	83.90	39.95	18.00
$m$	4.38	11.03	9.80



Figs 2 and 3 Weibull's diagram for static and dynamic cases (cast iron)

simplicity. This leads to a two parameters statistical approach and in the context equation (3) is used

$$P(K_{Ic}) = 1 - \exp[-\{K_{Ic}/K_0\}^m] \quad (3)$$

This method allows to calculate the average value  $\bar{K}_{Ic}$  according to the following formula

$$\bar{K}_{Ic} = K_0 \Gamma(1 + 1/m) \quad (4)$$

where  $\Gamma$  is the symbol of the gamma function. By introducing the variance, it is possible to describe scatter. The variance is given by

$$\sigma^2 = K_0^2 [\{\Gamma(1 + 2/m)\} - \{\Gamma(1 + 1/m)\}^2] \quad (5)$$

Experimental results are presented using the following presentation by transforming equation (3) according to

$$\ln(\ln[1/(1 - P(K_{Ic}))]) = m \ln(K_{Ic}) - m \ln K_0 \quad (6)$$

The plot of  $\ln(\ln[1/(1 - P(K_{Ic}))])$  versus  $\ln(K_{Ic})$  is a straight line of slope  $m$  (Figs 2 and 3). For each value of fracture toughness a probability of failure is obtained by the following procedure: for the  $N$  broken samples the individual fracture toughness  $K_{Ic(i)}$  values are ordered by increasing magnitude. After each individual value of rank  $i$  received a level of failure probability  $P(K_{Ic, i})$

equal to:

$$P(K_{Ic, i}) = i/(N + 1) \quad (7)$$

The plot of equation (6) gives, for the three materials, the parameters of the distribution ( $K_0, m$ ). These values are listed in Table 5 and an example of such a curve is given in Fig. 2.

### Discussion

For the two parameters Weibull distribution, we have the corresponding probability density function

$$f(K_{Ic}) = m/K_0 (K_{Ic}/K_0)^{m-1} \exp\{- (K_{Ic}/K_0)^m\} \quad (8)$$

To obtain a better fit of results and a comparison with the normal distribution, the relationship (8) becomes ( $S'$  standard deviation)

$$(K_{Ic}) = L C_w / S' \sqrt{2\pi} \exp[-1/2(K_{Ic} - \bar{K}_{Ic}/S')^2] \quad (9)$$

The constants  $C_w$  and the class with  $L$  are listed in Table 6. In Fig. 1 relative to the cast iron, we can notice that the Weibull distribution gives a better representation of the probability distribution, particularly for the 'tails'. This is a general conclusion which explains the big popularity of the Weibull empirical formula. We can also notice that the average values calculated with the Weibull distribution are greater than those calculated with the normal distribution.

The Weibull shape parameter  $m$  is generally greater under static loading. The table giving Weibull parameters for three materials confirms the fact. For A 508 Cl 3 the dynamic modulus becomes 2.81 times smaller than the static one; for the cast iron 2.6 times, and for the magnesium alloy 1.2 times.

This increase of scatter has previously been considered as a consequence of the multi-defect activation process which appears in dynamic.

The multi-activation process was described by Kalthoff (11). The critical stress-versus crack size curve is such that the product  $\sigma_c \sqrt{a}$  is equal to a constant in the static case. By dynamic loading the curve reaches an asymptotic value for a long defect. A large range of defects can be activated simultaneously with the same critical stress. This is the so-called multi-activation

Table 6 Values of class width and  $C_w$  constants

Tests	Constants	A 508 Cl 3	Cast iron	GA 3Z1
Static	$L$	11.48	1.24	0.90
	$C_w$	45	36	18
Dynamic	$L$	2.79	3.39	1.15
	$C_w$	65	36	30

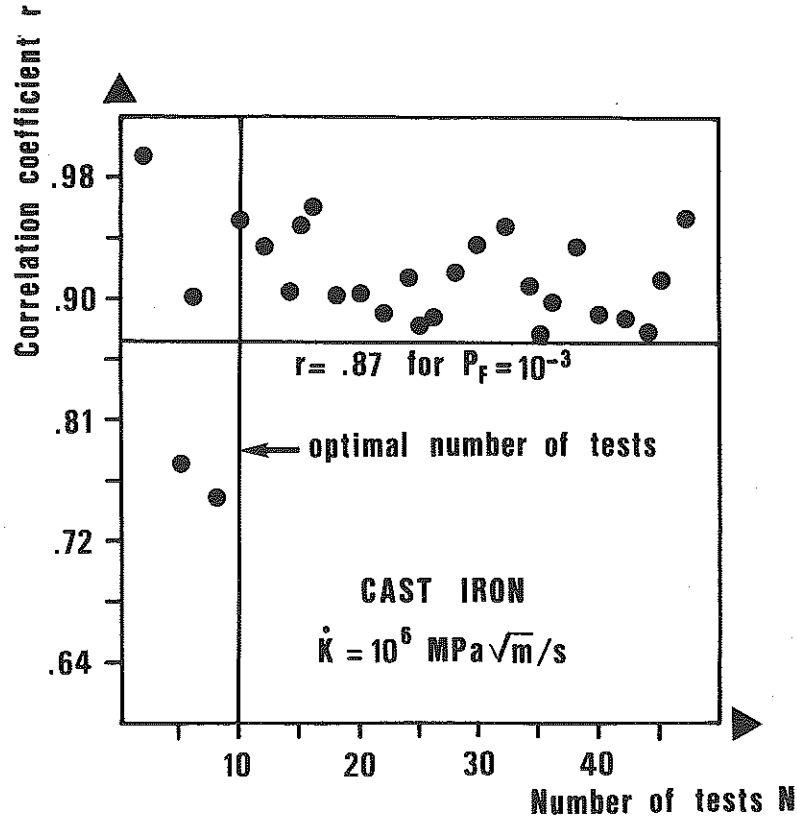


Fig 4 Determination of minimum test number required for a reliable determination of fracture toughness

process leads to a larger scatter band of fracture toughness values. Evidences of the multi-activation process have been seen on ceramics by (3) and on propellants by (12). These evidences are of two categories direct and indirect.

Direct evidences can be obtained by picture analysis of the broken surface. In ceramics and in propellants the number of broken grains strongly increases with the loading rate. This phenomenon was attributed to the activation of porosity between grains.

Indirect evidence of this process is the increase of scattering and the decreasing of the fracture surface roughness.

Table 7 Minimum tests number to obtain a reliable estimation of fracture toughness

Numbers of tests	A 508 Cl 3	Cast iron	GA3Z1
Static	6	5	5
Dynamic	7	10	12

In the case of cast iron, steels, and magnesium alloys direct evidences of this multi-activation where not detected from SEM investigation. Only scatter of results and change in the fracture roughness was seen.

Another thing leads one to think that this can be attributed to a change in the fracture process. For dynamic fracture of ceramics, the Weibull plot is not a straight line. We can also notice in Figs 2 and 3 that the same phenomenon appears for cast iron (but not for steel and magnesium alloys).

In the case of cast iron, two values of Weibull modulus were obtained:  $m = 16.40$  and  $m = 3.50$ . The evidence of this two slope representation is more sensitive to the number of tests than to the scale of the  $x$  axis of the diagram.

For this reason, it is necessary to determine the minimum number of tests required for a correct representation. An empirical value of 0.87 for the correlation coefficient  $r$  was chosen to determine this number which varies from 5 to 12 according to the material and loading rate. This value was chosen by looking at the graph correlation coefficient versus number of tests and can be considered as a sort of engineering estimation of lower bound of  $K_{Ic}$ .

### Conclusion

By increasing the loading rate from 1 to  $10^6$  MPa $\sqrt{m/s}$  the scattering of fracture toughness increases. This was previously seen on ceramics and propellants and confirmed in the present paper on magnesium, cast iron, and steel.

A change in the fracture process could not be detected on the fracture surface as it was seen on ceramics and propellants. Only analogy with the increasing value of Weibull modulus and a two slope probability distribution leads one to think that the same phenomenon occurs.

Another promising way for evidence of the multi-activation defect process is the roughness of the failure surface measurement.

### References

- (1) LACOURT, G. (1986) *Etude de la tenacité et du comportement dynamique en fonction de la température de différents types d'aciers*, Thèse, Université de Metz.
- (2) NEVIÈRE, R. (1989) *De l'application des critères énergétiques globaux de la mécanique de la rupture à l'étude des explosifs et propulseurs solides composites*, Thèse, Université de Metz.
- (3) TOLBA, B. (1988) *Approche statistique de la tenacité sous sollicitations dynamique: application aux matériaux céramiques et métalliques*, Thèse, Université de Metz.
- (4) GARNIER, V. *Etude de la tenacité et du comportement de quatre aciers sous différentes conditions de température et de vitesse de déformation*, Thèse Université de Metz.
- (5) PELISSIER-TANON, A. (1984) Improvements to PWR vessel fracture analysis methods, *ICF6*, New Delhi, pp. 691-706.
- (6) KONECA *et al.* (1986) Rôle du modificateur sur les mécanismes de rupture par chocs de la fonte à graffite vermiculaire, *Mémoires et Etudes Scientifiques de la Revue de Metallurgie*.
- (7) WILSHAW, T. R., RAU, C. A., and TETELMAN, A. S. (1968) *Engng Fracture Mech.*, 1, 191.
- (8) SPINK, G. M., WORTHINGTON, P. J., and HEAD, P. T. (1972) Post yield fracture mechanics. *Mater. Sci. Engng*, 10, 129-137.
- (9) HICKERSON, J. P. (1977) Experimental confirmation of the  $J$ -integral as a thin section fracture criterion, *Engng Fracture Mech.*, 9, 75-85.
- (10) DAMBRINNE, B. (1981) Thèse, Université de Compiègne.
- (11) KALTHOFF, J. P. and SHOCKEY, J. (1977) Short pulse fracture mechanics, *J. Appl. Phys.*, 48, 986.